



Energy research Centre of the Netherlands

Study of a thermoacoustic-Stirling engine

M.E.H. Tijani
S. Spoelstra
G.A. Poignand

Paper presented at Acoustics '08, Paris, France, June 29-July 4, 2008



Study of a thermoacoustic-Stirling engine

H. Tijani, S. Spoelstra and G. Poignand

Energy research Centre of the Netherlands (ECN), Westerduinweg 3, 1755 LE Petten,
Netherlands
tijani@ecn.nl

A Stirling cycle thermoacoustic engine is developed and performance measurements are performed. The engine uses thermal power to generate acoustic power. It consists mainly of three parts: a thermodynamic part consisting of a regenerator, two heat exchangers, and a thermal buffer tube; an acoustic network consisting of an acoustic compliance and an inertance; and a resonator. The thermodynamic part and the acoustic network are placed in a torus configuration. The hot heat exchanger is placed on the top of the torus so that the shape and size of the hot heat exchanger can be designed or chosen independently of the regenerator dimensions. Two different resonator types of about a $\frac{1}{4}$ -wave length have been tested during the study of the engine. The first resonator forms a too heavy load for the engine and could not be loaded with an RC-acoustic load. A second resonator is designed and built that has less loss than the first one. The performance measurements with the second resonator show that the engine at its most efficient operating point generates 190 watt of acoustic power with an efficiency of 22.5 %, corresponding to 36 % of Carnot.

1 Introduction

The history of heat-driven oscillations, known today as thermoacoustics, is rich and old [1, 2]. In 1850, Soundhauss studied experimentally such oscillations which have been observed for centuries by glass-blowers when blowing a hot bulb at the end of a cold tube [1]. In 1887, Lord Rayleigh gave a quantitative explanation for the oscillations in his classic work on sound [3]. It is only in the 1940's that the first formal theoretical study of thermoacoustics started [4]. In 1969, Rott continued the theoretical work which resulted in a successful linear theory of thermoacoustics [5, 6, 7].

In the 1960's many varieties of the Soundhauss tube (engine) have been conceived and built to improve the sound production. In 1958, Morrison invented an engine with two heat exchangers but no stack to produce electricity from sound [8]. In 1962, Carter et al. is the first that used a stack to improve the performance [9]. In 1968, Feldman et al. [2] also studied an engine with a stack but without heat exchangers. Although these engines had different concepts they all used standing-wave phasing and all meet Rayleigh criterion for the heat-driven oscillations.

Until about 1999, most efforts in thermoacoustics have been focused on the development and understanding of standing-wave thermoacoustic systems [10,11]. These systems are relatively simple to design and build but they are intrinsically irreversible because of the imperfect thermal contact between the working medium and the stack. This means that these systems cannot achieve high thermodynamic performance. The most efficient standing-wave engine built up to day had an efficiency of 20 % [12].

In 1979, Ceperley showed that the time phasing between pressure and gas velocity in the regenerator of a Stirling system is that of a traveling acoustic wave [13]. However, the first attempt of Ceperley to build a traveling-wave thermoacoustic engine did not succeed. This was due mainly to the viscous losses in the regenerator as a consequence of the low acoustic impedance (high velocity). It is only in 1998 that the first working traveling-wave engine was demonstrated but at low efficiency [14].

The breakthrough in the development of thermoacoustic engines was realized by Backhaus et al. [15] in 1999 when they developed a traveling-wave thermoacoustic engine that achieved a measured thermal efficiency of 30 %, corresponding to 41 % of Carnot efficiency. They used a torus-shaped compact acoustic network to create the traveling-wave phasing necessary for the operation in a Stirling cycle. The high efficiency is achieved only after the Gedeon and Rayleigh streaming were reduced to a minimum level.

In spite of the progress and improvements, thermoacoustic technology still did not find its way to industry. At ECN efforts have been made to map possible applications which may be of interest for the industry. One of these applications is the use of a thermoacoustic heat pumps driven by a thermoacoustic engines to upgrade waste heat. This may be a solution to the reuse of the huge quantities of waste heat which are released to the environment that cannot be reused, mostly because the temperature level is too low. The work presented in this paper reports part of these efforts.

The aim of this paper is to present a study of a 1 kW thermal power traveling-wave (Stirling) thermoacoustic engine. The design, development, and performance measurements of the engine will be presented.

The remaining of this paper is organized as follows: Section 2 is devoted to the characteristics and design of the engine. In section 3, a description of the engine is given. Section 4 explains the measurement techniques. Section 5 is devoted to the performance measurements. In the last section some conclusions are drawn.

2 Characteristics of the engine

The aim is to design, build and test a compact traveling-wave thermoacoustic engine with a thermal power of about 1 kW. The engine uses the thermal power produced by electric cartridge heaters to generate acoustic power. Helium gas at an average pressure of 40 bar is used as the working medium at the operation frequency of 150 Hz. The thermoacoustic-Stirling engine consists mainly three parts: a thermodynamic part consisting of a regenerator, two heat exchangers, and a thermal buffer tube; an acoustic network consisting of an acoustic compliance and an inertance; and a $\frac{1}{4}$ -wavelength resonator. The regenerator is the heart of the engine where the thermoacoustic conversion process takes place. The heat exchangers take care of the heat exchange between the engine and the exterior. The torus-shaped acoustic network contains the regenerator, the heat exchangers, a feedback inertance, and an acoustic compliance. This network creates the traveling-wave phasing necessary to operate in a Stirling cycle and feeds back part of the acoustic power produced by the engine. The resonator functions as a pressure vessel for the working gas, and determines the resonance frequency.

The hot heat exchanger is placed at the top of the torus, similar to that used by Backhaus et al. [16]. In this way the shape and size of the hot heat exchanger can be designed or chosen independently of the shape and size of the regenerator. This gives some freedom in the design

especially when the operating temperature of the engine is low as is the case for a waste heat driven engine.

Unlike standing-wave thermoacoustic engines, traveling-wave engines function like an amplifier. So, acoustic power has to be continuously fed at the ambient side of the engine so that it can be amplified by the temperature difference across the regenerator. The regenerator and heat exchangers function like an acoustic flow resistance in the acoustic network.

The optimal design of the engine is realized with the computer code DeltaE [17]. In the next section the engine will be described.

3 Description of the engine

A schematic illustration of the thermoacoustic-Stirling engine is shown in Fig 1. Beginning at the hot heat exchanger and anti-clockwise around the torus are the regenerator, the ambient heat exchanger, the compliance, the inertance, the junction to the resonator and the thermal buffer tube. A description of the different parts will be given in the following subsections.

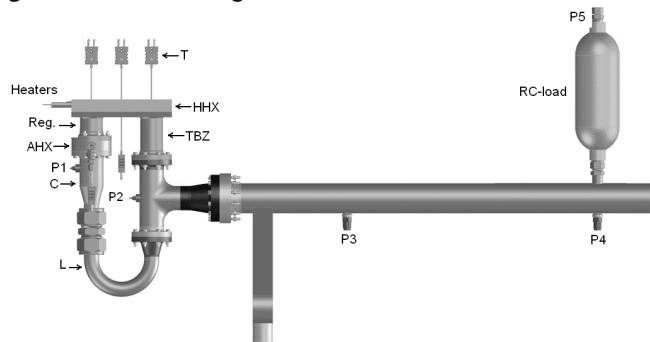


Fig. 1 Illustration of the thermoacoustic-Stirling engine

3.1 Hot heat exchanger

The hot heat exchanger is placed at the top of the loop. It is made of high temperature resistant steel and contains small passages for the helium gas. It consists of two rectangular thick plates 20 cm long and 9 cm wide. In the plates, comb patterns are cut so that when the two plates are stacked and brazed small rectangular channels are formed. The upper thick plate contains also holes where four cartridge heaters can be inserted. The lower plate contains two circular ports with a diameter of 4.8 cm where the regenerator cylindrical housing and the thermal buffer tube can be brazed. These two ports are centred at 12 cm apart which corresponds to the peak-peak displacement of the gas in the channels at 10 % drive ratio. The thermal power is supplied by four cartridge heaters of 300 W each. The heat enters the system by conduction and reaches the helium gas oscillating in the small channels. The hot heat exchanger contains also some holes where thermocouples can be placed for temperature measurements. The maximum operation temperature for the hot heat exchanger is 650 °C. The hot heat exchanger is indicated by “HHX” in Fig.1.

3.2 Regenerator

The regenerator consists of a 5.5 cm thick stack of 165-mesh twilled-weave stainless-steel screen punched at a diameter of about 4 cm. The diameter of the screen wire is 50 µm. The stack of screens is placed in a thin-wall tube (holder). The calculated hydraulic radius of the regenerator is 36.5 µm which is smaller than the helium’s thermal penetration depth (about 115 µm at 300 K). The regenerator is indicated by “Reg.” in Fig.1.

3.3 Ambient hot heat exchanger

The ambient heat exchanger consists of a circular aluminium block with 228 cylindrical channels drilled through it. The channels have a diameter of 1.5 mm and a length of 2 cm through which the helium gas oscillates. Water is flowing in annular channels around this block to carry away the heat rejected by the engine during operation. The ambient heat exchanger is indicated by “AHX” in Fig.1.

3.4 Acoustic network

The compact acoustic network used to create the local traveling-wave phasing and the high acoustic impedance in the regenerator consists of the resistance of the regenerator and heat exchangers, a compliance and a feedback inertance which are arranged in a torus configuration (c.f. Fig.1). The compliance consists of a volume of 120 cc and is indicated by “C” in Fig.1. The feedback inertance consists of a cylindrical tube of length 30 cm and a diameter of 2.5 cm, indicated by “L” in Fig.1. The torus is closed by a tee with an inner diameter of 4 cm, joining the inertance to the thermal buffer tube and to the resonator as shown in Fig.1. The thermal buffer tube consists of a stainless steel tube with a diameter of 4 cm and a length of 17 cm, indicated by “TBZ” in Fig.1.

3.5 Resonator

As shown in Fig.1, the resonator is attached to the torus at the T-junction between the thermal buffer tube and the inertance. Two different resonators of about a ¼-wave length have been tested during the study of the engine. The first resonator is made of stainless steel and it consists of a straight tube with a diameter of 5.5 cm and length of 2.3 m which ends in a cylindrical volume of 10 litres. The first test of the engine done with this resonator showed that the resonator forms a too heavy load for the engine which leads to a high operating temperature of the engine. To avoid this problem and to explore the possibility of loading the engine using an acoustic RC-load it was decided to build a second resonator with less acoustic losses. This second resonator consists of four sections. The first section is a cone with a length of 7.6 cm changing diameter from 4 to 5.5 cm. The second section is a straight tube with a diameter of 5.5 cm and length of 1 m. The third section is a cone with length 1.3 m an initial and final diameter of 5.5 and 16 cm. To explore the possibility of using different shapes for the conical part, PVC-blocks with the correct shape are placed inside a constant-diameter 6” pipe. The last section is a stainless steel tube with a diameter of 16 cm and length of 39 cm, terminating in a cap. Care has been taken to get

smooth transitions between the different parts. An RC acoustic load is attached to the 5.5 cm diameter resonator as shown in Fig.1. The variable acoustic RC-load consists of a 1-liter tank and an adjustable valve. The acoustic power dissipated in the variable acoustic load is a function of the valve setting. The end cap of the resonator contains the fill line.

The resonance frequency of the engine with the second resonator is higher than with the first one; 150 Hz instead of 110 Hz. This means that the performance of the engine will degrade.

4 Measurement techniques

The characterization of the performance of the engine requires knowledge of many quantities like temperatures, dynamic pressures at different locations of the system, heat powers at the hot and ambient heat exchangers, and acoustic power produced by the engine. In the following subsections, a description of the instrumentation used for the measurements and the expressions used to determine the different powers and performance are given.

4.1 Instrumentation

Several type-K thermocouples are used to measure the temperature at different locations of the engine and they are indicated by "T" in Fig.1. Five thermocouples with a diameter of 2 mm are placed in 5 holes drilled in the upper plate of the hot heat exchanger and one thermocouple in the middle of the lower plate to measure the temperature distribution. Three thermocouples with a diameter of 0.5 mm are placed on the wall of the regenerator housing to measure the temperature: one at the hot side, one at the centre, and one at the ambient side. The axial temperature profile along the regenerator is used to detect Gedeon streaming [16]. Three other 0.5 mm diameter thermocouples are placed equidistant on the wall of the thermal buffer tube. The temperature profile measured by these two thermocouples is used to detect the presence of either Rayleigh or jet-driven streaming [16]. Finally, two 2 mm-thick thermocouples are used to measure the inlet and outlet temperatures of the water stream cooling the ambient heat exchanger. Several pressure sensors are placed throughout the system. Two pressure sensors are located at the torus: one at the compliance and one at the resonator junction. Two pressure sensors are placed on the 5.5 cm diameter resonator to measure the acoustic power passing their midpoint (two-microphone method). One pressure sensor is placed in the compliance of the load. In Fig.1 the pressure sensors are indicated by "P".

4.2 Powers

The determination of the performance of the engine requires the knowledge of different powers and temperatures in the system. The acoustic pressure signal measurements are made with a lock-in amplifier. The thermocouples signals are read by a data logger and sent to a computer for record and display.

The thermal power input from the heaters is given by

$$\dot{Q}_h = VI \quad (1)$$

where V is the voltage across the heater, and I is the current. The regenerator, hot heat exchanger and the thermal buffer tube have been thermally insulated.

The heat extracted at the ambient side of the regenerator by cooling water flowing through the ambient heat exchanger is given by

$$\dot{Q}_a = \rho c_p U (T_{out} - T_{in}) \quad (2)$$

where ρ is the density of water, c_p is the specific heat, U is the volume flow rate of water, and T_{in} and T_{out} are the input and output temperatures of the water stream flowing through the ambient heat exchanger. The volume flow rate is measured with a turbine flow meter.

By reference to Fig., the acoustic power flowing past the midpoint of the two pressure sensors P_3 and P_4 is given by [18]

$$\dot{W}_{2mic} = \frac{A}{2\omega\rho_g\Delta x} \left[\left(1 - \frac{\delta_v}{r} \right) p_3 p_4 \sin \alpha + \frac{\delta_v}{2r} (p_3^2 - p_4^2) \right] \quad (3)$$

Where P_3 and P_4 are the amplitudes of the dynamic pressures measured by the two pressure sensors, Δx is the distance between the two transducers along the resonator, α is the time phase difference, ω is the angular frequency, ρ_g is the density of the gas, and δ_v is the viscous penetration depth.

The acoustic power dissipated in the RC-load is given by [18]

$$\dot{W}_{load} = \frac{\omega v}{2\gamma p_m} p_4 p_5 \sin \beta, \quad (4)$$

where P_4 and P_5 are the amplitudes of the dynamic pressures measured at the entrance of the load and in the compliance of the load respectively, β is the phase difference between P_4 and P_5 , ω is the angular frequency, v is the volume of the compliance of the load, p_m is the average pressure of the gas, and γ is the ratio of the isobaric to isochoric specific heats. The pressure transducer P_4 is placed at the port of the RC-load on the resonator and it is used for the two-microphone method and to measure the acoustic power dissipated in the load.

The acoustic power produced by the engine at the resonator junction is the sum of the acoustic power dissipated in the whole resonator and that dissipated in the RC-load.

The power measured by the two-microphone method is the sum of the acoustic power dissipated in the resonator section to right of the midpoint of the two-microphones and the acoustic power dissipated in the load

$$\dot{W}_{2mic} = \dot{W}_{res} + \dot{W}_{load}. \quad (5)$$

Because of the difficulty of the two-microphone method and its sensitivity to the microphone placement, phase difference, and flow conditions, this method is verified by expression (5). This means that if the two-microphone measurements are accurate, the plot of \dot{W}_{2mic} versus \dot{W}_{load} at constant drive ratio should be a line of slope one and the intercept at $\dot{W}_{load} = 0$ gives \dot{W}_{res} . The acoustic power at the

junction to the resonator W is deduced from W_{2mic} by extrapolation using the DelatE model of the engine.

4.3 Performance indicators

The performance of the engine is given by

$$\eta = \frac{\dot{W}}{Q_h}, \quad (6)$$

where W is the acoustic power produced by the engine at the resonator junction.

The Carnot efficiency is the maximum theoretical performance of the engine and is given by

$$\eta_c = \frac{T_H - T_a}{T_H} \quad (7)$$

where T_H is the temperature of the hot heat exchanger measured by the thermocouple placed at middle of the lower side and T_a is the average temperature of the cooling water flowing through the ambient heat exchanger. The performance relative to Carnot is defined as the ratio

$$\eta_R = \frac{\eta}{\eta_C} \quad (8)$$

The experimental results will be presented in the following section for several drive ratio's. The drive ratio is defined as the ratio of the dynamic pressure amplitude in the compliance and the mean pressure of the gas.

An elastic membrane is placed at the ambient heat exchanger to suppress Gedeon streaming. Two flow straighteners consisting of a Ni-foam sheet are placed at the ends of the thermal buffer tube to ensure that the flow at these locations is spatially uniform.

5 Experimental results

The measurements described in this paper are performed with the second resonator at a resonance frequency of 150 Hz.

In Fig. 2, the acoustic power output of the engine is plotted against the square of the drive ratio for the case where the resonator forms the only load for the engine. About 190 watt of acoustic power is dissipated in the resonator at a drive ratio of 7.1 %. To check the accuracy of the acoustic power measured by the two-microphone method, expression (5) is plotted in Fig.3 for three drive ratio's namely 4, 5.8 and 7.1 %. For the drive ratio of 7.1 % the engine could not be loaded, so only one point is measured corresponding to the acoustic power dissipated in the resonator. The solid lines are linear fits to experimental data. The slope is about 1 which gives confidence in the measurements.

The performance of the engine as a function of the temperature of the hot heat exchanger as defined in expression (6) is given in Fig.4. The performance increases slightly as function of the temperature of the hot heat exchanger.

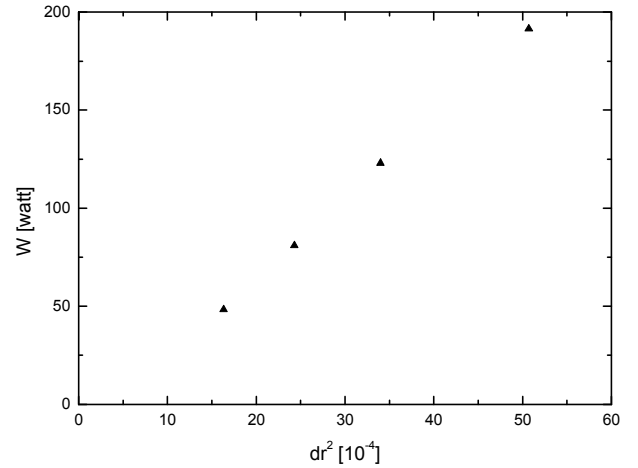


Fig.2 Acoustic power out of the engine as function of the square of the drive ratio. The resonator forms the only load.

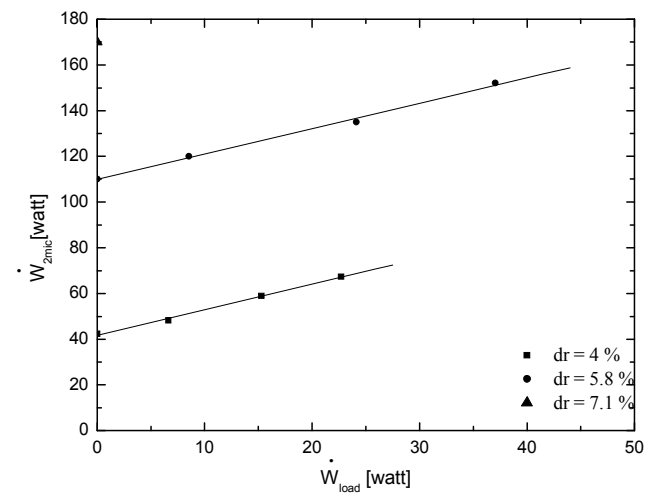


Fig.3 W_{2mic} versus W_{load} for different drive ratio's. The solid lines are linear fits to data.

The engine achieves a performance of 22.5 % at a drive ratio of 7.1 %, corresponding to 36 % of the Carnot efficiency. This relatively good performance is obtained in spite of the fact that the regenerator and acoustic network have originally been designed in combination with the first resonator (110 Hz). This means that the engine performs less. By adapting the design to the second resonator it is possible to improve the performance of the engine.

The heat transfer between helium gas and the hot heat exchanger is good because of the small channels. However, the small channels cause an appreciable pressure drop and hence acoustic power dissipation. Additionally, the relatively big area of the hot heat exchanger increases the heat leak to the environment.

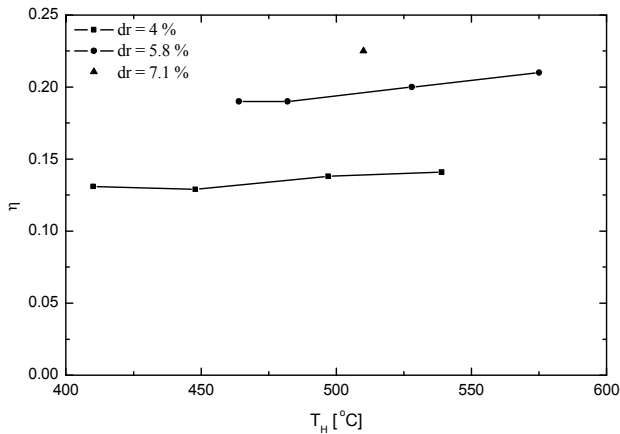


Fig. 4 Performance of the engine as function of the temperature of the hot heat exchanger for different drive ratio's.

6 Conclusion

A traveling-wave thermoacoustic engine with an external hot heat exchanger is designed, built and performance measurements have been performed. The engine generates 190 watt of acoustic power with an efficiency of 22.5 %, corresponding to 36 % of Carnot. The performance of the engine can be improved by redesigning the acoustic network and regenerator to match the frequency of the second resonator.

The small and long channels in the hot heat exchanger ensure a good heat exchange with helium gas but they cause also an appreciable pressure drop and hence acoustic power dissipation. An improvement of the design of the hot heat exchanger can also improve the performance.

Acknowledgments

This work has been funded by SenterNovem (Dutch agency for sustainable development and innovation) within the EOS-LT program.

References

- [1] C. Sondhauss, "Ueber die Schallschwingungen der Luft in erhitzten Glas-Rohren und in gedeckten Pfeifer von ungleicher Weite", *Ann. Phys.* 79, 1 (1850).
- [2] K.T. Feldman, Jr., "Review of the literature on Sondhauss thermoacoustic phenomena", *J. Sound Vib.* 7, 71-82 (1968).
- [3] Lord Rayleigh, "The theory of sound", 2nd edition, Vol.2, Sec.322 (Dover, New York, 1945).
- [4] H.A. Kramers, "Vibration of gas column", *Physica* 15, 971-984 (1949).
- [5] N. Rott, "Damped and thermally driven acoustic oscillations in wide and narrow tubes", *Z. angew. Math. Phys.* 20, 230-243 (1969).
- [6] N. Rott, "thermally driven acoustic oscillations, part II: Stability limit for helium", *Z. angew. Math. Phys.* 24, 54- (1973).
- [7] N. Rott, "thermally driven acoustic oscillations, part III: second-order heat flux", *Z. angew. Math. Phys.* 26, 43- (1975).
- [8] W.A. Marrison, "Heat-controlled acoustic wave system", U.S. patent No.2,836,033, 1958
- [9] R.L. Carter, M. White, and A.M. Steele, (Private communication of Atomics international Division of North American Aviation Inc., 1962).
- [10] G. W. Swift, "Analysis and performance of a large thermoacoustic engine", *J. Acoust. Soc. Am.* 92, 1515-1563 (1992).
- [11] M.E.H. Tijani, J.C.H. Zeegers, and A.T.A.M. de Waele "Design of a thermoacoustic refrigerators". *Cryogenics* 42, 49-57 (2002).
- [12] K. M. Godshalk, C. Jin, Y.G. Kwong, E.L. Hershberg, G.W. Swift, and R. Radebaugh, "Characterization of 350 Hz Thermoacoustic driven orifice pulse tube refrigerator with measurements of the phase of the mass flow and pressure. *Adv. Cryogenics Eng.*, 41, 1411-1418 (1996).
- [13] P.H. Ceperley, 'A pistonless Stirling engine-the traveling wave heat engine', *J. Acoust. Soc. Am.*, 66, 1508-1513 (1979).
- [14] T. Yazaki, A. Iwata, and T. Maekawa, "Traveling wave thermoacoustic heat engine in looped tube" *Phys. Rev. Lett.*, 81, 3128-3131 (1998).
- [15] S. Backhaus, G.W. Swift, "A thermoacoustic Stirling heat engine: Detailed study", *J. Acoust. Soc. Am.*, 107, 3148-3166 (2000).
- [16] S. Backhaus, E. Tward, and M. Petach, "travelling-wave Thermoacoustic electric generator", *App. Phys. Lett.* 85, 1085-1087, (2004)
- [17] W. Ward, G.W. Swift, "Design Environment for Low Amplitude Thermoacoustic Engine", *J. Acoust. Soc. Am.*, 95, 3671 (1994).
- [18] A.M. Fusco, W.C. Ward, G.W. Swift, "Two-sensor power measurement in lossy ducts", *J. Acoust. Soc. Am.*, 91, 2229-2235 (1992).